

## Plasma diagnostics during microwave plasma synthesis of graphene nanosheets

M. Snirer, J. Toman, V. Kudrle, O. Jašek, J. Faltýnek, J. Jurmanová

*Masaryk University, Brno, Czech Republic*

### **Introduction**

There exists wide range of methods to prepare advanced carbon materials like carbon nanotubes (CNT), nanofibres, graphene, nanoribbons or nanoflakes [1]. Among them, the plasma based techniques do not generally need a metallic catalyst or substrate but they require specific conditions such as sufficiently high energy of atomic and molecular species supplied to the growth zone and balanced carbon influx. Operating pressure of plasma environment has significant influence on the formation of nanoparticles and nanopowders [2] i.e. nanoparticle nucleation and growth, nanoparticle charging and agglomeration.

Recently, as an alternative to liquid exfoliation preparation of graphene nanosheets, it was shown that ethanol decomposition in microwave plasma led to successful formation of graphene nanosheets [3]. This methods was further investigated by Tatarova and Tsyganov [4] using microwave plasma surface wave discharge at atmospheric pressure in Ar/ethanol gas mixture. By further analysis and modelling they found that C<sub>2</sub> molecule promotes nucleation and growth of graphene and atomic C leads to deposition of amorphous and sp<sub>3</sub> phase.

In this work we study the influence of deposition conditions, especially a pressure, on the formation of carbon nanosheets. We previously showed that gas pressure has significant influence on the plasma synthesis of iron oxide based nanopowders [5, 6].

### **Experimental**

Carbon nanostructures were synthesized using surface wave driven microwave plasma. The experimental setup is shown in fig. 1. Plasma was sustained by microwave generator (Muegge) operating at 2.45 GHz with output power varied in range 350–550 W. The generator was connected to a standard waveguide system: water-cooled circulator, EB tuner, surfaguide [7] as the wave launching plasma applicator, and movable short at the end.

Discharge was ignited in fused silica tube (20 mm external and 16 mm internal diameter) placed vertically in the surfaguide. Argon was used as a main working gas with flow rates  $Q_{\text{main}}$  varying in range 1000–1400 sccm. Synthesis is based on plasma decomposition of the ethanol precursor. The vaporised precursor is introduced to the discharge using separate flow  $Q_{\text{mix}}$  of argon as a carrier gas, in a range 28–84 sccm, passing through bubbler with liquid ethanol. Gas

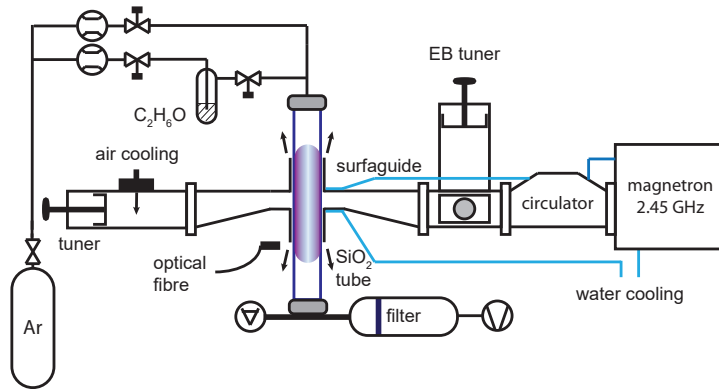


Figure 1: Experimental set-up.

flow rates were measured by Bronkhorst mass flow controllers.

In the case of the synthesis at low pressures reaction chamber was continuously evacuated using rotary vane oil pump for pressures lower than 8 kPa or dry diaphragm pump for pressures in the range 10-40 kPa. The operation was also carried out at atmospheric pressure, i.e. without any pumping.

Optical emission spectra were recorded by Jobin-Yvon Triax 550 spectrometer (1200 gr/mm, 3600 gr/mm) with LN<sub>2</sub> cooled CCD detector. Fused silica optical fibre ending 10 cm from the tube was used to collect plasma emission in different positions along the axis.

At the bottom end of the discharge tube there was placed a fine steel mesh filter to collect products of the synthesis. The samples were characterised by Raman spectroscopy (HORIBA LabRAM HR Evolution system with 532 nm laser) and by scanning electron microscopy (Tescan MIRA3 with Schottky field emission electron gun).

## Results and discussion

The overview spectrum of argon-ethanol plasma was measured at position 1 cm below the launcher (downstream the excitation zone), see fig. 2. The spectrum is dominated by molecular vibrational bands of C<sub>2</sub> (d<sup>3</sup>Π<sub>g</sub>-a<sup>3</sup>Π<sub>u</sub>) Swan system (400-550 nm) and violet CN (B<sup>2</sup>Σ<sup>+</sup>-X<sup>2</sup>Σ<sup>+</sup>) system (380-390 nm). Emission of the CN (which comes from small impurities) was used for temperature measurements. Experimental spectra were compared with simulated ones (see fig. 3) using Massive OES software [8] and vibrational temperature was calculated. Because the vibrational bands overlap, only (v',v'') = (0,0) band is recommended to use for the rotational temperature calculation [9].

In pure argon the surface wave discharge has typical appearance – long diffuse plasma column for low pressure and multiple short filaments for higher pressures. Presence of ethanol reduced plasma length to few centimetres. Different ratios of Ar:ethanol were investigated by changing

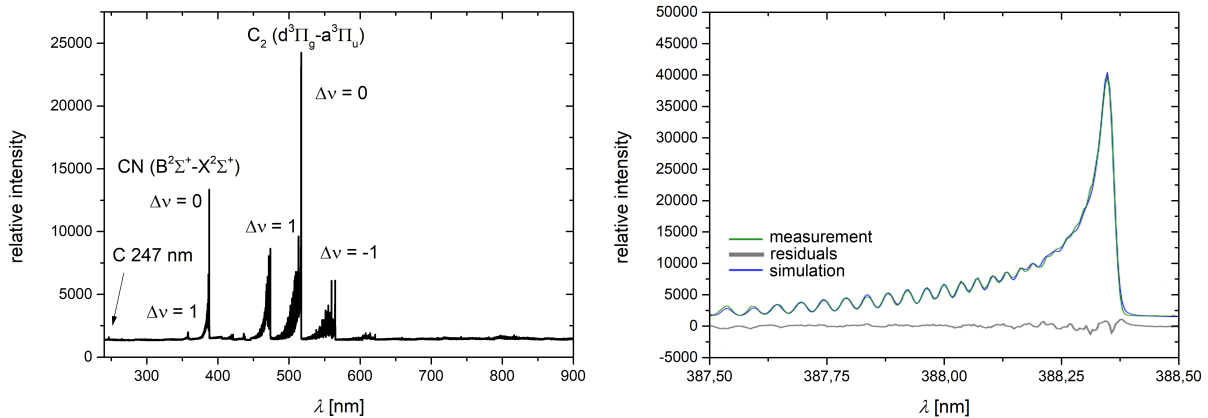


Figure 2: Typical OES spectrum of Ar-ethanol plasma.  $Q_{\text{main}} = 1400$  sccm,  $Q_{\text{mix}} = 56$  sccm,  $Q_{\text{main}}/Q_{\text{mix}} = 25$ ,  $p = 99$  kPa, 550 W. Figure 3: CN (v', v'') = (0,0) spectrum.  $Q_{\text{main}} = 1400$  sccm,  $Q_{\text{mix}} = 56$  sccm,  $Q_{\text{main}}/Q_{\text{mix}} = 25$ ,  $p = 99$  kPa, 550 W.

their respective flows  $Q_{\text{main}}$ ,  $Q_{\text{mix}}$ . Higher amount of ethanol lead to formation of intense green axial filament both at middle and atmospheric pressure conditions. Thermalisation depends on pressure as can be seen in fig. 4 by comparing values of rotational and vibrational temperatures. Spatial measurements showed increase in rot. temperature after passing through surfaguide e.g. for atmospheric pressure from 3000-3500 K (upstream) to 3500-4000 K (downstream). Higher amount of ethanol leads to increased emission intensity of C<sub>2</sub> molecule compared to atomic C, see fig. 5. Electron density in the filament was determined using MW interferometry and its typical value was in range  $2-8 \cdot 10^{17} \text{ m}^{-3}$  depending linearly on the input power.

There were considerable differences in plasma parameters and in properties of synthesised material between atmospheric pressure and lower pressure conditions. To obtain structural and quality characterisation of prepared carbon nanostructures, the Raman spectroscopy was used [10, 11]. Analyses showed presence of typical D ( $1330 \text{ cm}^{-1}$ ), G ( $1580 \text{ cm}^{-1}$ ) and 2D ( $2680 \text{ cm}^{-1}$ ) carbon peaks. Observed ratios of D/G peaks and 2D/G peaks suggest, that material synthesised at lower pressure conditions was predominantly composed by amorphous phase but at atmospheric pressure it contained few-layered graphene nanosheets.

SEM morphology analysis supports these results as it showed a presence of spherical nanoparticles (20 nm diameter) at lower pressure conditions, while at atmospheric pressure one may observe the graphene sheets with dimensions of several hundreds of nanometers.

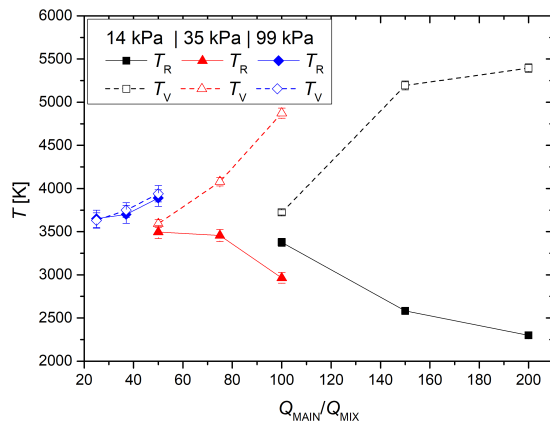


Figure 4: Comparison of rotational and vibrational temperatures of CN radical for different flow ratios  $Q_{\text{main}}/Q_{\text{mix}}$  in different pressure regions for 550 W.

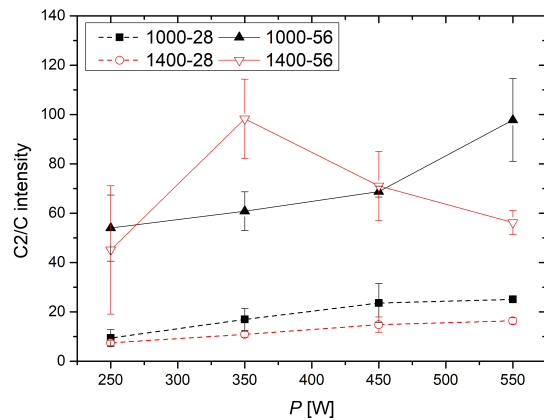


Figure 5: Evolution of optical emission intensity ratios of  $C_2(0,0)/C(247 \text{ nm})$  for different MW power and  $Q_{\text{main}}/Q_{\text{mix}}$  ratios at atmospheric pressure.

## Conclusion

Influence of the amount of ethanol admixture in different pressure conditions was investigated during plasma synthesis of graphene. Both higher amount of ethanol and operating pressure led to faster thermalization and favourable decrease in  $C_2$  dissociation. In that case the deposited material shifted from amorphous carbon to few-layered graphene nanosheets.

## Acknowledgement

This work was supported by the Czech Science Foundation under project No. 18-08520S and in part by the project LO1411 (NPU I) funded by Ministry of Education, Youth and Sports of Czech Republic.

## References

- [1] Ferrari, A. C., Bonaccorso, F., Falko, V., *Nanoscale*, **7**(11), 4598(2015)
- [2] D. Vollath, *Journal of Nanoparticle Research*, **10**(1), 39(2008)
- [3] Dato, A., Radmilovic, V., Lee, Z., et al. *Nano letters*, **8**, 7(2008)
- [4] Tysganov, D., et al. *Plasma Sources Science and Technology*, **25**(1), 015013(2015)
- [5] David B., Pizurova N., Schneeweiss O., et al. *Journal of Physics Conference*, **303**, 012090(2011)
- [6] David B., Pizurova N., Schneeweiss O., et al. *Journal of nanoscience and nanotechnology*, **12**, 9277(2012)
- [7] Moisan, M., Zakrzewski, Z., *J. Phys. D: Appl. Phys.*, **24**, 1025(1991)
- [8] Voráč, J., Synek, P., Potočnáková, et al. *Plasma Sources Science and Technology*, **26**(2), 025010(2017)
- [9] Moon, S.Y., et al. *Journal of applied physics*, **105**, 053307(2009)
- [10] Ferrari, Andrea C. *Solid state communications*, **143**, 47(2007)
- [11] Ni, Zhenhua, et al. *Nano Research*, **1**(4), 273(2008)